Hindawi Publishing Corporation
EURASIP Journal on Wireless Communications and Networking
Volume 2007, Article ID 59608, 11 pages
doi:10.1155/2007/59608

Research Article

Multi-Satellite MIMO Communications at Ku-Band and Above: Investigations on Spatial Multiplexing for Capacity Improvement and Selection Diversity for Interference Mitigation

Konstantinos P. Liolis, Athanasios D. Panagopoulos, and Panayotis G. Cottis

Wireless & Satellite Communications Group, School of Electrical and Computer Engineering, National Technical University of Athens (NTUA), 9 Iroon Polytechniou Street, Zografou, Athens 15780, Greece

Received 28 August 2006; Revised 2 March 2007; Accepted 13 May 2007

Recommended by Alessandro Vanelli-Coralli

This paper investigates the applicability of multiple-input multiple-output (MIMO) technology to satellite communications at the Ku-band and above. After introducing the possible diversity sources to form a MIMO matrix channel in a satellite environment, particular emphasis is put on satellite diversity. Two specific different topics from the field of MIMO technology applications to satellite communications at these frequencies are further analyzed: (i) capacity improvement achieved by MIMO spatial multiplexing systems and (ii) interference mitigation achieved by MIMO diversity systems employing receive antenna selection. In the first case, a single-user capacity analysis of a satellite 2×2 MIMO spatial multiplexing system is presented and a useful analytical closed form expression is derived for the outage capacity achieved. In the second case, a satellite 2×2 MIMO diversity system with receive antenna selection is considered, adjacent satellite cochannel interference on its forward link is studied and an analytical model predicting the interference mitigation achieved is presented. In both cases, an appropriate physical MIMO channel model is assumed which takes into account the propagation phenomena related to the frequencies of interest, such as clear line-of-sight operation, high antenna directivity, the effect of rain fading, and the slant path lengths difference. Useful numerical results obtained through the analytical expressions derived are presented to compare the performance of multi-satellite MIMO systems to relevant single-input single-output (SISO) ones.

1. INTRODUCTION

Multiple-input multiple-output (MIMO) technology has recently emerged as one of the most significant technical breakthroughs in modern digital communications due to its promise of very high data rates at no cost of extra spectrum and transmit power [1, 2]. Wireless communication can be benefited from MIMO signaling in two different ways: *spatial multiplexing* and *diversity*. In the former case, independent data is transmitted from separate antennas, and aiming at maximizing throughput (i.e., linear capacity growth with the number of antennas can be achieved). In the latter case, the same signal is transmitted along multiple (ideally) independently fading paths aiming at improving the robustness of the link in terms of each user BER performance. These advantages have been largely responsible for the success of MIMO both as a research topic and as a commercially viable technology in terrestrial communications [1, 2].

The appealing gains obtained by MIMO techniques in terrestrial networks generate a further interest in investigating the possibility of applying the same principle in satellite networks, as well. However, the underlying differences between the terrestrial and the satellite channels make such applicability a non straightforward matter and, therefore, a rather challenging subject. In this case, one of the fundamental problems is the difficulty of generating a completely independent fading profile over the space segment. In satellite communications, due to the huge free space losses along the earth-space link, line-of-sight (LOS) operation is usually deemed a practical necessity. However, this is not the typical case in terrestrial communications where rich scattering and non-LOS environments with multipath propagation

are encountered. Thus, placing multiple antennas on a single satellite does not seem a suitable choice in order to exploit the MIMO channel capabilities. In fact, the absence of scatterers in the vicinity of the satellite leads to an inherent rank deficiency of the MIMO channel matrix. Therefore, at a first glance, the applicability of MIMO technology to satellite channels does not seem well justified.

The objective of this paper is in line with some other recent research efforts [4–8, 12–16] casting further light in this regard. These studies have been mainly concerned with the possible diversity sources that can be exploited in satellite communications to form a MIMO *matrix* channel. A categorization of these diversity sources follows.

(i) *Site diversity*, where multiple cooperating terminal stations (TSs), sufficiently separated from each other, are in communication with a single satellite. So far, it has only been studied as an efficient rain fade mitigation technique at the Ku (12/14 GHz), Ka (20/30 GHz), and Q/V (40/50 GHz) frequency bands because of its very low achievable spatial correlation due to rain [3]. However, due to the enormous slant path lengths associated, the required separation distance between the multiple TSs to ensure ideally independent fading profile is of the order of several km, which rather hinders its practical interest in MIMO applications.

(ii) *Satellite* (or *orbital*) *diversity*, where multiple satellites, sufficiently separated in orbit to provide (ideally) independently fading channels, communicate with a single TS equipped with either multiple antennas or even a single multiple-input antenna. So far, it has been studied mostly as an efficient rain fade mitigation technique in Ku-, Ka-, and Q/V-band satellite communications [3] and, also, recently, as a candidate to form satellite MIMO matrix channels at high (i.e., Ku, Ka, and Q/V) [4, 5] as well as at low frequency bands, such as L (1/2 GHz) and *S* (2/4 GHz) [6–8]. Also, it is worthwhile noting that it is already successfully employed in the continental US digital audio radio services (DARS), mobile systems, Sirius and XM satellite radio, operating at the *S*-band [9]. Satellite diversity provides a rather practical solution of reasonable complexity since the multiple received signals at the single TS can easily be combined due to the colocation of the antennas. However, an inherent problem of this scheme, apart from the costly utilization of multiple satellites, is the asynchronism of the multiple transmitted signals at the TS receiver, which comes as a result of the propagation delay difference due to the wide separation between the satellites. A similar problem is dealt with and solutions are proposed in several papers mainly concerning distributed sensor networks, such as in [10]. To the authors' knowledge, for the more complicated satellite case—due to the much larger and variable delay difference—the only relevant solution proposed so far is reported in [5].

(iii) *Polarization diversity*, where a single dual-orthogonal polarized satellite communicates with a single TS equipped with a dual-orthogonal polarized antenna. Its principle is based on the polarization sensitivity of the reflection and diffraction processes, which causes random signal fading at the TS receiver. It represents a solution of rather practical interest due to the recent developments in MIMO compact antennas (see, e.g., [11]) which allow for compact MIMO setups. It has already been examined as a promising solution to shape MIMO channels in *S*-band land mobile satellite communications [7, 12–16]. Its main advantage over satellite diversity is the elimination of any additional cost associated with the utilization of multiple satellites. It also bypasses the asynchronism problem associated with the distributed nature of satellite diversity. However, it can be disadvantageous to satellite diversity especially in satellite networks operating at high-frequency bands (i.e., Ku, Ka, and Q/V), which are affected by the highly correlated rainfall medium and, also, in case of large blockages resulting in hard system failures (i.e., on/off channel phenomena). Moreover, as concluded in [13], polarization diversity can only increase the transmission rate of a satellite communication system by a factor of two, whereas in multi-satellite systems, satellite diversity can result in m-fold capacity increase, where m is the number of satellites occupied.

This paper focuses particularly on dual-satellite MIMO communication systems employing satellite diversity. Moreover, emphasis is put on the less congested high-frequency bands, such as Ku and above. At these frequencies, multipath propagation is insignificant. However, by virtue of satellite diversity, MIMO can be considered to effectively exploit the rainfall spatial inhomogeneity instead. A physical 2×2 MIMO satellite channel model is assumed taking into account the relevant propagation phenomena, such as clear LOS operation, high antenna directivity, rain fading, and rainfall spatial inhomogeneity [3, 17]. This model is flexible and can be applied on a global scale since it has physical inputs obtained by regression fitting analysis on the ITU-R rainmaps [18] and is based on general assumptions about the rain process [17]. Moreover, it incorporates the general case of an *ordered* MIMO satellite channel (due to the slant path lengths difference). To this end, the resulting propagation delay offset is assumed to be properly taken into account at the TS receiver. A possible practical solution to this problem might be the one implemented in [5] according to which matched filters are first applied to the received signals for the detection of the propagation delay offset, which is then fed to a timing aligner. Subsequently, the proposed timing aligner eliminates the delay offset by adjusting the timing of a signal parallel-to-serial converter. The study of more efficient solutions to the asynchronism problem associated with satellite diversity, although rather challenging, is out of the scope of this paper and will be the subject of a future work.

In the first part of this work, emphasis is put on a satellite 2×2 MIMO *spatial multiplexing* system and on its possible capacity improvement with respect to the relevant SISO system. The term "spatial multiplexing" refers to the transmission of independent data streams from the multiple separate satellites [1, 2]. Well-known results obtained from the MIMO literature [19, 20] are applied here for the capacity analysis of such a 2×2 MIMO system. The figure of merit used to characterize the resulting MIMO fading channel is the *outage capacity* [1], for which an analytical closed form expression is provided. Note that such analytical expressions are extremely hard to obtain even in the well-established field

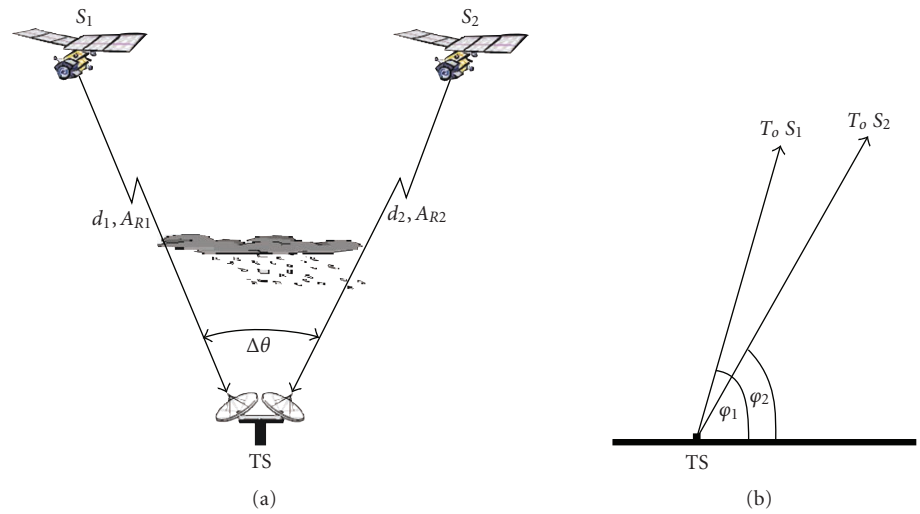

FIGURE 1: (a) Configuration of a dual-satellite 2×2 MIMO channel. Individual satellites S_1 and S_2 transmit either independent data streams (MIMO spatial multiplexing system, Section 3) or the same signal over the multiple (ideally) independently fading paths (MIMO diversity system, Section 4), (b) associated elevation angles.

of MIMO theory due to the intractability of the outage capacity distribution [2].

In the second part, a satellite 2×2 MIMO *diversity* system employing receive antenna selection is examined, and issues specifically related to cochannel interference (CCI) are addressed from a propagation point of view. The term "diversity" refers to the transmission of the same signal over the multiple (ideally) independently fading paths [1, 2]. Receive antenna selection is a low-cost, low-complexity approach to benefit from many of the advantages of MIMO technology while, at the same time, bypassing the multiple RF chains associated with multiple antennas at the receiver, which are costly in terms of size, power, and hardware [21]. The interference analysis presented here is quite different from conventional communication-oriented approaches followed in standard MIMO theory [1]. Attention is paid to the CCI problems arising on the forward link of such a 2×2 MIMO satellite system due to *differential rain attenuation* from an adjacent satellite [22]. To deal with the statistical behaviour of the signal-to-interference ratio (SIR) introduced by the rainfall spatial inhomogeneity, the concept of *unacceptable interference probability*[1] [23, 24] is employed here. An analytical prediction model concerning the interference mitigation achieved by the proposed satellite 2×2 MIMO diversity system is provided.

The rest of the paper is organized as follows. Section 2 presents the channel model adopted for MIMO satellite communications at the Ku-band and above. Section 3 provides a communication-based capacity analysis for a satellite 2×2 MIMO spatial multiplexing system. A propagation-oriented analysis for the possible interference mitigation achieved by a satellite 2×2 MIMO diversity system with receive antenna selection is presented in Section 4. Useful numerical results obtained for both the above satellite MIMO applications considered are provided in Section 5. Section 6 concludes the paper.

2. MIMO SATELLITE CHANNEL MODEL

Figure 1 depicts the configuration of a dual-satellite MIMO communication channel at the Ku-band and above. The TS is equipped with two colocated highly directive antennas and communicates with two satellites, S_1 and S_2, subtending an angle $\Delta\theta$ to the TS, large enough that the spatial correlation due to rain along the relevant slant paths is as low as possible. The normalized radiation pattern of each TS antenna, denoted by $G_R(\cdot)$, is compatible with the ITU-R specifications [25] and is shown in Figure 2.[2] The lengths of slant paths S_i-TS are denoted by d_i $(i = 1, 2)$ and the random variables (RVs) associated with the respective rain induced attenuations (in dB) are denoted by A_{Ri} $(i = 1, 2)$. In general, the two slant paths S_i-TS have different elevation angles denoted by ϕ_i $(i = 1, 2)$, respectively.

Assuming that clear LOS between the TS and each satellite S_i exists, that each TS antenna is at boresight with the corresponding satellite S_i $(i = 1, 2)$ and that rain attenuation is the major fading mechanism, the path gain for each S_i-TS link is modeled as

$$g_i \propto G_R(0^\circ) \cdot d_i^{-2} \cdot 10^{-A_{Ri}/10} \quad (i = 1, 2). \tag{1}$$

[1] Note that the concept of the "unacceptable interference probability (UIP)" in this paper is exactly the same as that of the "acceptable interference probability (AIP)" employed in [23, 24]. Their only difference concerns their nomenclature.

[2] Note that the analyses presented hereafter are quite general and, therefore, may incorporate other TS antenna radiation patterns, as well.

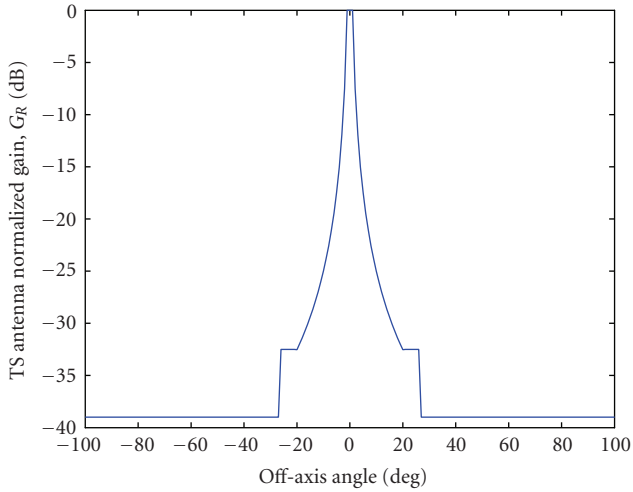

Figure 2: Normalized radiation pattern of each TS antenna compatible with ITU-R specifications [25].

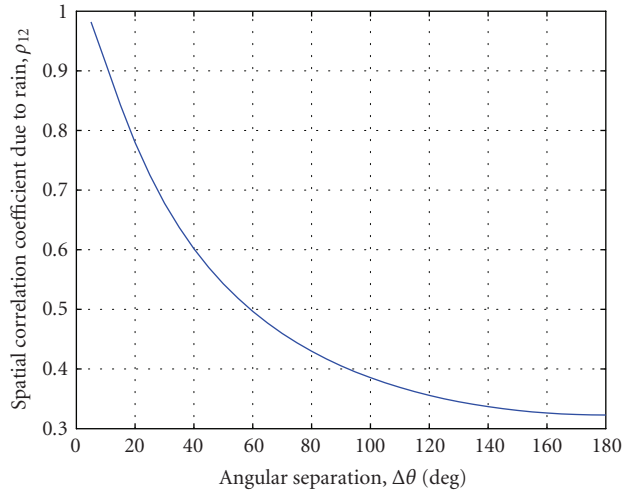

Figure 3: Spatial correlation coefficient due to rain ρ_{12} versus angular separation $\Delta\theta$ for a dual-satellite MIMO channel operating in Atlanta, GA, at the Ka-band with satellite elevation angles $\phi_1 = 45^\circ$ and $\phi_2 = 40^\circ$.

Hence, the total path loss along each S_i-TS link (in dB) is

$$A_i = \mathrm{FSL}_i + A_{Ri} \quad (i = 1, 2), \tag{2}$$

where $\mathrm{FSL}_i = 10\log_{10}(4\pi d_i f/c)^2$ is the free space loss along each link, c the speed of light, and f the operating frequency. Note that the fundamental assumptions concerning the modeling of the rain attenuation RVs A_{Ri} $(i = 1, 2)$ are the same as those analytically presented in [17]. The convective raincell model employing Crane's assumptions is used for the description of the vertical variation of the rainfall structure [17]. Based on this assumption, if $\Delta\theta$ is sufficiently large, the spatial correlation coefficient between the RVs A_{Ri} is relatively low and, thus, an (ideally) decorrelated MIMO satellite channel is possible. To this end, an illustrative quantitative example is presented in Figure 3, which depicts the spatial correlation coefficient due to rain ρ_{12} versus $\Delta\theta$ for a dual-satellite MIMO channel operating in Atlanta, GA, USA at the Ka-band with satellite elevation angles $\phi_1 = 45^\circ$ and $\phi_2 = 40^\circ$.

Based on the above and, also, assuming frequency nonselective fading, the resulting MIMO channel matrix $\mathbf{H}$ is given by

$$\mathbf{H} = \begin{bmatrix} h_{11} & h_{12} \\ h_{21} & h_{22} \end{bmatrix} = \begin{bmatrix} \sqrt{g_1}\exp\left(\dfrac{j2\pi d_1 f}{c}\right) & 0 \\ 0 & \sqrt{g_2}\exp\left(\dfrac{j2\pi d_2 f}{c}\right) \end{bmatrix}. \tag{3}$$

The diagonal structure of $\mathbf{H}$ is due to the high directivity of the TS antennas and the large value of $\Delta\theta$. In MIMO terminology, channels with diagonal $\mathbf{H}$ matrix are known as *parallel MIMO channels*. Further details about such channels can be found in [26]. Moreover, as opposed to standard MIMO theory [1, 2], $\mathbf{H}$ is not normalized here (i.e., *ordered* MIMO channel) due to the different slant path lengths d_i $(i = 1, 2)$. Finally, the assumption of independent identically distributed (i.i.d) elements of $\mathbf{H}$, often made in conventional terrestrial MIMO systems, cannot be made here, since there is a relatively high spatial correlation due to rain.

3. SATELLITE MIMO SPATIAL MULTIPLEXING SYSTEM: CAPACITY ANALYSIS

In this Section, the two satellites S_i $(i = 1, 2)$ depicted in Figure 1 are assumed to transmit different and independent data streams (i.e., *spatial multiplexing* is investigated). The channel $\mathbf{H}$ is considered perfectly known to the TS receiver (via training and tracking), while at the transmit side, both satellites are assumed to have no channel knowledge. In the absence of channel state information (CSI) at the transmit side, equal power allocation to the two satellites is a reasonable and rather practical choice, due to the distributed nature of the system. Therefore, from the standard MIMO theory, the following well-known formula for the capacity (in bps/Hz) of MIMO channels is adopted [19, 20]:

$$C = \log_2 \det\left(\mathbf{I}_2 + \frac{P_T}{2N_0}\mathbf{H}\mathbf{H}^H\right) = \sum_{i=1}^{2}\log_2\left(1 + \frac{P_T}{2N_0}\lambda_i\right), \tag{4}$$

where $\mathbf{I}_2$ is the 2×2 identity matrix, P_T the total average power available at the transmit side,[3] N_0 the noise spectral

[3] Note that P_T is the sum transmit power of all transmitting satellites S_i regardless of their number. This means that in both the dual-satellite MIMO case and the single satellite SISO case, the total available transmit power is constant and equal to P_T. This is ensured employing the normalization factor "2" in (4), which allows for a fair comparison between the relevant MIMO and SISO cases.

density at the TS receiver input, and λ_i $(i = 1, 2)$ the positive eigenvalues of the matrix $\mathbf{HH}^H$ (the superscript ^{H} stands for conjugate transposition).

Taking into account the channel modeling assumptions, (4) is written as

$$C = \sum_{i=1}^{2} \log_2 \left(1 + 0.5\mathrm{SNR}_{\mathrm{CS}i} 10^{-A_{Ri}/10}\right), \tag{5}$$

where $\mathrm{SNR}_{\mathrm{CS}i}$ $(i = 1, 2)$ are the nominal SNR values under clear sky conditions. Based on the path gain model given in (1), the $\mathrm{SNR}_{\mathrm{CS}i}$ values (in dB) are related through

$$\mathrm{SNR}_{\mathrm{CS1}} - \mathrm{SNR}_{\mathrm{CS2}} = 20 \log_{10}\left(\frac{d_2}{d_1}\right). \tag{6}$$

Equation (5) provides an expression for the *instantaneous capacity* of a deterministic 2×2 MIMO channel $\mathbf{H}$. However, since the rainfall introduces slow fading and stochastic behaviour over the channel $\mathbf{H}$, the appropriate statistic measure to characterize the resulting fading channel is the *outage capacity* defined by [1]

$$P(C \le C_{\mathrm{out,q}}) = q, \tag{7}$$

where $C_{\mathrm{out,q}}$ is the information rate guaranteed for $(1-q)100\%$ of the channel realizations.

Consider the RV transformation

$$u_i = \frac{\left[\ln(A_{Ri}) - \ln(A_{m_{Ri}})\right]}{S_{a_{Ri}}} \quad (i = 1, 2) \tag{8}$$

which relates the lognormal rain attenuation RVs A_{Ri} $(i = 1, 2)$ to the normalized normal RVs u_i $(i = 1, 2)$. Substituting (5) into (7) and after some straightforward algebra, the following analytical closed form expression for the outage capacity is obtained:

$$P(C \le C_{\mathrm{out,q}}) = \frac{1}{2} \int_{u_A}^{+\infty} du_1 f_{U_1}(u_1)\, \mathrm{erfc}\left(\frac{u_B - \rho_{n12} u_1}{\sqrt{2(1-\rho_{n12}^2)}}\right) = q, \tag{9}$$

where $\mathrm{erfc}(\cdot)$ is the complementary error function, $f_{U_1}(u_1)$ the probability density function (pdf) of the normal distribution, ρ_{n12} the logarithmic correlation coefficient between the normal RVs u_i $(i = 1, 2)$ [17] and u_A, u_B are analytically given by

$$u_A = \Big[\ln\left(10\log_{10}(0.5\mathrm{SNR}_{\mathrm{CS2}}) - 10\log_{10}\left(2^{C_{\mathrm{out,q}}} - 1\right)\right) - \ln(A_{m_{R2}})\Big]/S_{a_{R2}}, \tag{10}$$

$$u_B = \Big[\ln\Big(10\log_{10}(0.5\mathrm{SNR}_{\mathrm{CS1}}) + 10\log_{10}\left(1 + 0.5\mathrm{SNR}_{\mathrm{CS2}} 10^{-A_{m_{R2}} \exp(u_1 S_{a_{R2}})/10}\right) - 10\log_{10}\left(2^{C_{\mathrm{out,q}}} - 1 - 0.5\mathrm{SNR}_{\mathrm{CS2}} 10^{A_{m_{R2}} \exp(u_1 S_{a_{R2}})/10}\right)\Big) - \ln(A_{m_{R1}})\Big]/S_{a_{R1}}. \tag{11}$$

The quantities $A_{m_{Ri}}$, $S_{a_{Ri}}$ $(i = 1, 2)$, encountered in (8)–(11), are the statistical parameters of the lognormal RVs A_{Ri} $(i = 1, 2)$ given by [17]

$$S_{a_{Ri}}^2 = \ln\left[1 + \frac{H_i}{L_{Di}^2}\left(\exp\left(b^2 S_r^2\right) - 1\right)\right] \quad (i = 1, 2),$$
$$A_{m_{Ri}} = a R_m^b L_{Di} \exp\left(\frac{b^2 S_r^2 - S_{a_{Ri}}^2}{2}\right) \quad (i = 1, 2), \tag{12}$$

where L_{Di} $(i = 1, 2)$ are the projections of the *effective path lengths* L_i $(i = 1, 2)$ [17] on the earth surface, H_i $(i = 1, 2)$ are spatial parameters related to each path of length L_{Di} $(i = 1, 2)$ which may be found in [17], and a, b are constants depending on the operating frequency f, the polarization tilt angle, the temperature, and the rainfall characteristics over the serviced area. R_m, S_r are the lognormal statistical parameters of the rainfall rate R (in mm/hr). A reliable database of rainfall statistics for any geographical location on earth is provided by ITU-R in [18] and is used throughout the present work as an input to the simulations performed in order to determine the values of R_m, S_r.

4. SATELLITE MIMO DIVERSITY SYSTEM WITH RECEIVE ANTENNA SELECTION: INTERFERENCE ANALYSIS

In this section, the two satellites S_i $(i = 1, 2)$ depicted in Figure 1 are assumed to transmit the same signal over the (ideally) independently fading paths S_i-TS $(i = 1, 2)$ (i.e., *diversity* is investigated). To alleviate the high cost and complexity associated with multiple RF chains, the dual-antenna TS receiver is equipped with only one RF chain and performs antenna selection, that is, the 2×2 MIMO satellite system assumed employs *receive selection diversity* [21]. Therefore, the TS receiver detects the signal related to the path with the highest SNR. Under the constraint of only one RF chain at the receiver, in order to know all SNRs simultaneously for optimal selection, a training signal in a preamble to the transmitted data is assumed. During this preamble, the TS receiver scans the two antennas, finds that one with the highest SNR, and selects it for reception of the next data burst. Thus, only a few more training bits are required instead of additional RF chains.

Particular emphasis is put on possible interference mitigation offered by the proposed satellite 2×2 MIMO diversity system. In this regard, a propagation-based analysis is performed which is quite different from conventional communication-oriented approaches followed in standard MIMO theory [1]. Specifically, the effect of rainfall on the interference analysis is taken into account and the *differential rain attenuation* related to an adjacent satellite is considered as the dominant cause of the SIR degradation [22]. Such an interference problem is further aggravated due to the spatial inhomogeneity of the rainfall medium. It constitutes a typical interference scenario, especially over congested urban areas, where the increased demand for link capacity and radio coverage imposes the coexistence of many satellite radio links over the same geographical and spectral area. In the following, an analytical prediction model is presented, which

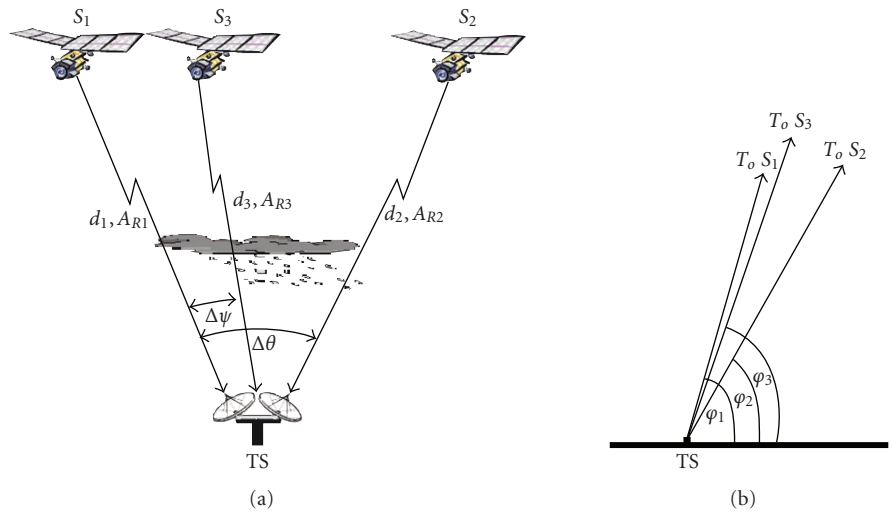

FIGURE 4: (a) Configuration of the satellite 2 × 2 MIMO diversity system assumed and the interference scenario on its forward link, (b) associated elevation angles.

quantifies the adjacent satellite CCI mitigation achieved by the proposed 2 × 2 MIMO system with respect to the corresponding SISO one.

Figure 4 depicts the configuration of the assumed interference scenario on the forward link of a satellite 2×2 MIMO diversity system operating at the Ku-band and above and employing receive antenna selection. The satellites S_1 and S_2 constitute the dual-satellite transmit part of the MIMO system also depicted in Figure 1. Another cochannel satellite (denoted by S_3), which may belong to either the same or to another satellite network, is close in orbit to S_1. Thus, CCI problems may arise on the forward link of the 2 × 2 MIMO satellite system. S_1 and S_3 subtend an angle $\Delta\psi$ to TS. The length of the slant path S_3-TS is denoted by d_3, while its elevation angle is ϕ_3. The RV associated with the rain induced attenuation along the interfering path S_3-TS (in dB) is denoted by A_{R3}.

Due to selection diversity at the TS receiver, the antenna with the maximum SNR is selected. In mathematical terms, the same statement is expressed as

$$\mathrm{SNR}_{\mathrm{out}} = \max\{\mathrm{SNR}_1, \mathrm{SNR}_2\} \Longleftrightarrow A_{\mathrm{out}} = \min\{A_1, A_2\}, \tag{13}$$

where $\mathrm{SNR}_i = \mathrm{SNR}_{\mathrm{CS}i} - A_{Ri}$ $(i = 1, 2)$ is the SNR at each TS antenna under rain fades and A_i $(i = 1, 2)$ the total path loss along each S_i-TS link $(i = 1, 2)$. $\mathrm{SNR}_{\mathrm{out}}$ corresponds to A_{out} which determines the output of the selection combiner at every instant. The proposed scheme requires only the knowledge of the wanted signals' channels at the receiver, whereas knowledge of the interferer's channel is not necessary. Moreover, no CSI is required at the transmit side. If M_d denotes the diversity system margin associated with the system availability p_{avail} (see the appendix), the satellite MIMO diversity system is considered available when the probabilistic event

$$\Omega = (A_{\mathrm{out}} < M_d) \tag{14}$$

is true. Assuming that

$$\Omega_i = (A_i < M_d, A_i < A_j) \quad ((i, j) = (1, 2), (2, 1)) \tag{15}$$

denotes the event that "the TS is serviced by the corresponding satellite S_i $(i = 1, 2)$," it becomes clear that, due to selection diversity,

$$\begin{aligned} \Omega &= \Omega_1 \cup \Omega_2, \\ \Omega_1 \cap \Omega_2 &= \varnothing. \end{aligned} \tag{16}$$

Therefore, the probability that the system is available (see the appendix) can be expressed as

$$P(\Omega) = P(\Omega_1) + P(\Omega_2). \tag{17}$$

While the satellite 2 × 2 MIMO diversity system is available (i.e., when *either* Ω_1 *or* Ω_2 are true), it might suffer from CCI originating from the adjacent satellite S_3. If SIR_d and r_d denote the SIR and the minimum acceptable SIR threshold of the MIMO diversity system, respectively (both measured at the output of the TS selection combiner), the probability of the event that "the system is interfered while being available" can be mathematically expressed based on the above considerations as

$$\begin{aligned} \mathrm{UIP}_d &= P(\mathrm{SIR}_d < r_d, \Omega) \\ &= P(\mathrm{SIR}_{d1} < r_d, \Omega_1) + P(\mathrm{SIR}_{d2} < r_d, \Omega_2) \\ &= P_1 + P_2, \end{aligned} \tag{18}$$

where UIP_d is the so-called *unacceptable interference probability* (UIP) [23, 24], and the quantities SIR_{di} $(i = 1, 2)$ are expressed (in dB) as

$$\mathrm{SIR}_d = \mathrm{SIR}_{di} = \mathrm{SIR}_{\mathrm{CSi}} - A_{Ri} + A_{R3} \quad (i = 1, 2). \tag{19}$$

In (19), $\mathrm{SIR}_{\mathrm{CSi}}$ $(i = 1, 2)$ is the nominal SIR value under clear sky conditions. In propagation terminology, $A_{Ri} - A_{R3}$

($i = 1, 2$) is known as the *differential rain attenuation* (DRA) [22]. Based on (19), when DRA becomes sufficiently large due to the spatial inhomogeneity of the rainfall medium, severe CCI problems may arise aggravating the SIR_d distribution on the forward link of the proposed satellite 2×2 MIMO diversity system. To this end, UIP_d is proposed as an efficient metric to deal with the statistical behaviour of the SIR_d and, together with r_d, they constitute a pair of design specifications concerning interference. Every user must comply with these specifications, given the QoS specified by the event Ω related to the system availability (see the appendix).

The quantities $\mathrm{SIR}_{\mathrm{CSi}}$ ($i = 1, 2$) encountered in (19) are given by

$$\mathrm{SIR}_{\mathrm{CSi}} = \mathrm{SIR}_i^* - G_R(\theta_i) \quad (i = 1, 2), \tag{20}$$

where θ_i ($i = 1, 2$) are the off-axis angles formed by the interfering link S_3-TS and the wanted links S_i-TS ($i = 1, 2$) in the radiation pattern of the TS antennas. From Figure 4, it follows that $\theta_1 = \Delta\psi$ and $\theta_2 = \Delta\theta - \Delta\psi$. Also, in (20), SIR_i^* ($i = 1, 2$) are the relevant SIR values of the interfered links S_i-TS ($i = 1, 2$) when $\theta_i = 1^\circ$, and correspond to the nominal CCI levels. Based on the channel model assumed, their interrelationship is defined through (6) by simply substituting the $\mathrm{SNR}_{\mathrm{CSi}}$ by SIR_i^*.

Extending the transformation given in (8) to include also the interfering link S_3-TS (i.e., for $i = 1, 2, 3$) and making the channel modeling assumptions, the probabilities P_i ($i = 1, 2$) encountered in (18) after some straightforward algebra are evaluated, that is,

$$P_i = \int_{u_{Ci}}^{u_{Di}} du_1 \int_{u_1}^{+\infty} du_2 f_{U_1U_2}(u_1, u_2) \times \left[1 - \frac{1}{2}\,\mathrm{erfc}\left(\frac{u_{Ei} - \mu_{3/1,2}}{\sqrt{2}\sigma_{3/1,2}}\right)\right] \quad (i = 1, 2), \tag{21}$$

where $f_{U_1U_2}(u_1, u_2)$ is the pdf of the two-dimensional joint normal distribution.

For $i = 1, 2$, the rest of the parameters encountered in (21) are

$$u_{Ci} = \frac{[\ln(x_{di}) - \ln(A_{m_{Ri}})]}{S_{a_{Ri}}},$$

$$x_{di} = \begin{cases} 0, & r_d > \mathrm{SIR}_{\mathrm{CSi}}, \\ (\mathrm{SIR}_{\mathrm{CSi}} - r_d)\cos\phi_i, & \mathrm{SIR}_{\mathrm{CSi}} + \mathrm{FSL}_i - M_d < r_d \le \mathrm{SIR}_{\mathrm{CSi}}, \\ (M_d - \mathrm{FSL}_i)\cos\phi_i, & r_d \le \mathrm{SIR}_{\mathrm{CSi}} + \mathrm{FSL}_i - M_d, \end{cases}$$

$$u_{Di} = \frac{[\ln((M_d - \mathrm{FSL}_i)\cos\phi_i) - \ln(A_{m_{Ri}})]}{S_{a_{Ri}}},$$

$$u_{Ei} = \left[\ln\left(\left(\frac{\exp(u_i S_{a_{Ri}})A_{m_{Ri}}}{\cos\phi_i} - \mathrm{SIR}_{\mathrm{CSi}} + r_d\right)\cos\phi_3\right) - \ln(A_{m_{R3}})\right] / S_{a_{R3}}. \tag{22}$$

$A_{m_{Ri}}$, $S_{a_{Ri}}$ ($i = 1, 2, 3$) are analytically given in (12). Furthermore, $\mu_{3/1,2}$ and $\sigma_{3/1,2}$ are the statistical parameters of the conditional distribution of the normal RV u_3 given the other two normal RVs u_1, u_2 and can be expressed in terms of the logarithmic correlation coefficients $\rho_{nij}((i, j) = (1, 2), (1, 3), (2, 3))$ as [17, 27]

$$\mu_{3/1,2} = \frac{\rho_{n13} - \rho_{n12}\rho_{n23}}{1 - \rho_{n12}^2}u_1 + \frac{\rho_{n23} - \rho_{n12}\rho_{n13}}{1 - \rho_{n12}^2}u_2,$$
$$\sigma_{3/1,2}^2 = \frac{1 - \rho_{n12}^2 - \rho_{n13}^2 - \rho_{n23}^2 + 2\rho_{n12}\rho_{n13}\rho_{n23}}{1 - \rho_{n12}^2}. \tag{23}$$

5. NUMERICAL RESULTS AND DISCUSSION

The previous analyses have been applied for the prediction of possible capacity improvement and interference mitigation achieved by the proposed satellite 2 × 2 MIMO spatial multiplexing and diversity systems, respectively, and for comparison to the relevant SISO cases. To this end, the baseline configuration scenario considers a TS located in Atlanta, GA, and communicating with geostationary satellites $S_1(\phi_1 = 45^\circ)$ and $S_2(\phi_2 = 40^\circ)$. The angular separation assumed is $\Delta\theta$=40°, which results in a spatial correlation coefficient of rain attenuation $\rho_{12} = 0.6$ (see Figure 3). Moreover, regarding the interference scenario, an adjacent geostationary satellite $S_3(\phi_3 = 45^\circ)$, separated from S_1 by $\Delta\psi$=10°, is considered to cause CCI problems on the forward link of the satellite 2 × 2 MIMO diversity system.

First, the validity of the proposed analytical model in (9), predicting the outage capacity achieved by a satellite 2 × 2 MIMO spatial multiplexing system, is numerically verified. The effect of various geometrical and operational system parameters on the outage capacity distribution is also examined.

Figure 5 shows the dependence of the 1% outage capacity of the assumed 2 × 2 MIMO satellite system on the SNR.[4] The baseline configuration scenario is adopted, whereas the operating frequency band assumed is Ka (i.e., $f = 20$ GHz). For the sake of comparison, the capacity of the relevant SISO system is also plotted. Together with the analytical results obtained from the analytical closed form expression in (9), Monte Carlo simulation results are also plotted for verification. The agreement observed between the analytical and the simulation results is very good over the whole SNR range. As can be seen, the difference between the relevant MIMO and SISO curves diminishes at very low SNR levels while it becomes significant as the SNR increases. As an illustration, for SNR = 10 dB, the spectral efficiency achieved by the MIMO system is 4.84 bps/Hz, whereas the one achieved by the SISO system is 3.23 bps/Hz. This constitutes, approximately, a 50% increase in user data rate obtained by MIMO spatial multiplexing. For SNR = 20 dB, the respective performance figures obtained are 10.95 bps/Hz and 6.41 bps/Hz corresponding to, approximately, a 71% increase in user data

[4] Note that the clear sky SNR of strong eigenmode, $\mathrm{SNR}_{\mathrm{CS1}}$, has been particularly considered. However, due to the enormous slant path lengths associated, the resulting difference between $\mathrm{SNR}_{\mathrm{CSi}}$ ($i = 1, 2$) is minimum see (6) and, therefore, any of the two $\mathrm{SNR}_{\mathrm{CSi}}$ can be used as x-coordinates.

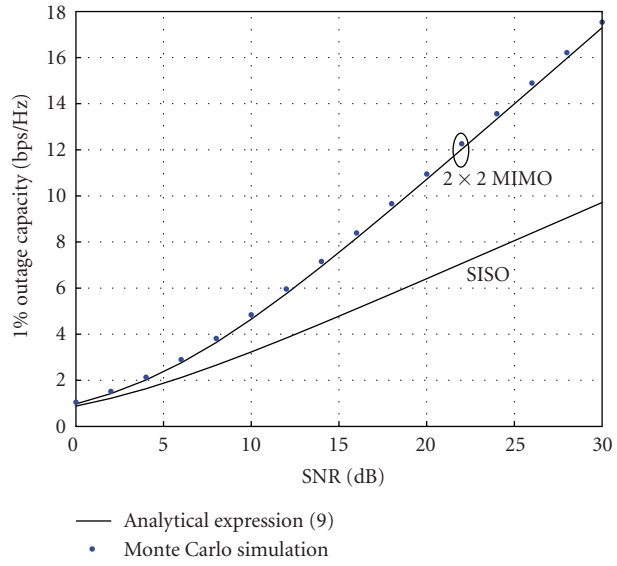

Figure 5: 1% outage capacity versus SNR for a satellite 2×2 MIMO spatial multiplexing system. Relevant SISO case is also plotted for comparison. Verification of analytical closed form expression in (9) through Monte Carlo simulation.

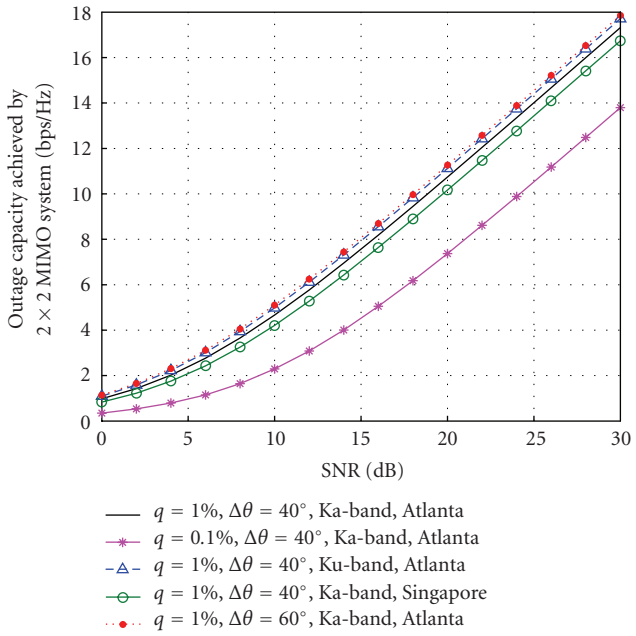

Figure 6: Outage capacity versus SNR for a satellite 2 × 2 MIMO spatial multiplexing system. Effect of capacity outage probability q, angular separation $\Delta\theta$, operating frequency f, and climatic conditions over the serviced area.

rate. Therefore, the capacity gain obtained by the proposed satellite 2 × 2 MIMO spatial multiplexing system over the SISO system turns out to be significant for no additional transmit power or bandwidth expenditure.

Figure 6 shows the dependence of the outage capacity achieved by a satellite 2 × 2 MIMO spatial multiplexing system on the SNR, the angular separation $\Delta\theta$, the operating frequency f, the capacity outage probability q, and the climatic conditions over the serviced area. All the results presented here have been obtained employing (9). The baseline configuration scenario is adopted. The rest of the relevant parameters assumed as well as the deviations from the baseline scenario are indicated on Figure 6. As can be seen, as either q decreases or f increases or as the rain conditions over the serviced area become heavier, the rain fading becomes more severe and, therefore, the outage capacity achieved by the 2 × 2 MIMO satellite system decreases. Moreover, as the angular separation $\Delta\theta$ increases (from 40° to 60°), the spatial correlation coefficient due to rainfall medium ρ_{12} decreases correspondingly (from 0.6 to 0.5, see Figure 3), and the outage capacity achieved increases.

In the following, the proposed analytical model in (21) predicting the interference mitigation achieved by a satellite 2 × 2 MIMO diversity system with receive antenna selection is numerically verified. The effect of various geometrical and operational system parameters on the forward link SIR distribution is also examined.

Figure 7 shows the dependence of the UIP of the assumed 2 × 2 MIMO satellite system on the SIR, the system availability p_{avail}, and the operating frequency band. Particularly, two different values of system availability, $p_{\text{avail}} = 99.9\%$ and 99.99%, and two different operating frequencies, $f =$ 12 GHz and 20 GHz, are assumed. For the sake of comparison, the UIP of the relevant SISO systems is also plotted. The baseline configuration scenario is adopted. The nominal CCI level assumed is $\text{SIR}_{\text{I}}^{*} = 20$ dB, whereas the rest of the parameters encountered in the interference analysis are indicated on Figure 7. It is obvious that, due to rain, an SIR degradation is observed for the same UIP level, which becomes more severe as either p_{avail} or f increases. This further indicates that satellite systems operating at higher availabilities or at higher-frequency bands are more sensitive to interference. The SIR improvement achieved by the satellite 2 × 2 MIMO diversity system over the SISO one is significant, especially for high p_{avail} and high f. As an illustration, for UIP = 0.001%, the interference mitigation obtained is 0.67 dB at the Ka-band and for a 99.9% availability, 1.60 dB at the Ku-band and for a 99.99% availability, and 3.52 dB at the Ka-band and for a 99.99% availability.

Figure 8 quantifies the SIR improvement achieved by a satellite 2 × 2 MIMO diversity system employing receive antenna selection with respect to the relevant SISO one. Specifically, the difference (in dB) between the respective SIR thresholds achieved at the TS receiver input for UIP = 0.001% is plotted versus the angular separation $\Delta\theta$. Two areas with different climatic conditions are considered, Atlanta, GA, and Athens, Greece. The operating frequency, system availability, and nominal CCI level assumed are 20 GHz, 99.99%, and $\text{SIR}_{\text{I}}^{*} = 20$ dB, respectively, while the rest of the parameters are the same as those of the baseline configuration scenario. As $\Delta\theta$ increases, the interference mitigation level achieved becomes higher. Moreover, it can easily be observed that the SIR improvement obtained in Atlanta,

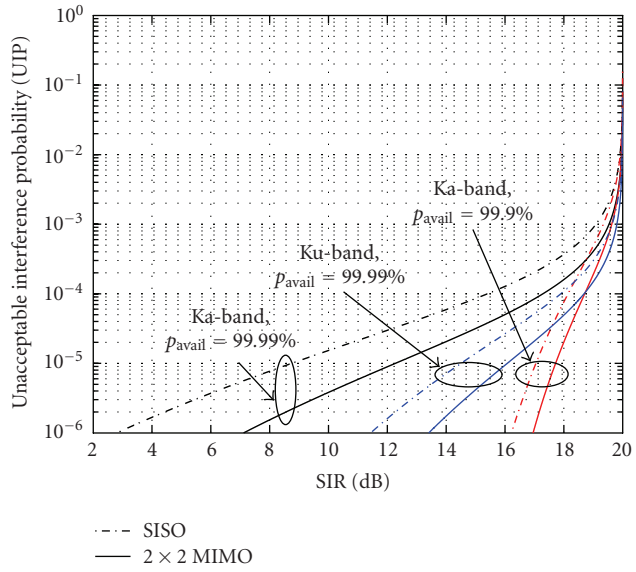

Figure 7: UIP versus SIR for a satellite 2 × 2 MIMO diversity system employing receive antenna selection. Relevant SISO case is also plotted for comparison. Effect of system availability p_{avail}, operating frequency f, and rain climatic conditions over the serviced area.

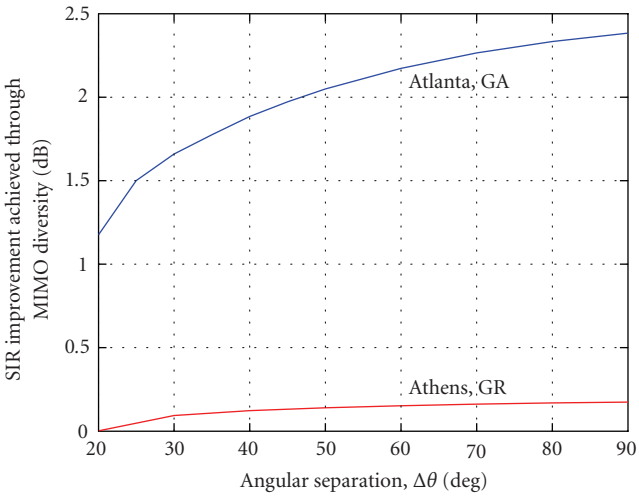

Figure 8: SIR improvement achieved by a satellite 2 × 2 MIMO diversity system with receive antenna selection over the relevant SISO system versus angular separation $\Delta\theta$. Effect of rain climatic conditions over the serviced area.

GA, is much higher than that in Athens, Greece, due to the corresponding heavier rain conditions.

For various obvious reasons, there is a tendency to place satellites in orbit close to each other. Due to the increased CCI, adjacent satellite networks cannot usually operate under certain SIR specifications. The proposed MIMO diversity system may overcome this problem by adequately increasing SIR in the presence of adjacent CCI. To demonstrate this, a satellite 2 × 2 MIMO diversity system together with its relevant SISO case are considered in Figure 9. The input parameters assumed are the same as those in the baseline configuration scenario, with the exception of a different angular separation $\Delta\psi$, that is, $\Delta\psi = 5°$ is now assumed. Operation of the system at the Ka-band and for a 99.99% availability is considered. To obtain the necessary QoS for UIP = 0.001%, suppose that an SIR threshold of 10 dB must be overcome. In the SISO case, when the angular separation between the wanted satellite S_1 and the adjacent interfering one S_3 is $\Delta\psi = 5°$, an SIR level of 11.2 dB is obtained for UIP = 0.001%, thus satisfying the QoS requirement. If the interfering satellite S_3 is closer in orbit to S_1, so that their angular separation is reduced to $\Delta\psi = 4°$, the SIR level in the SISO case falls down to 9.8 dB, thus failing to satisfy the QoS requirement. Employing the proposed 2 × 2 MIMO satellite system, the SIR achieved when $\Delta\psi = 4°$ is 11.32 dB, thus remaining above the QoS threshold. This is another advantage of the proposed satellite MIMO diversity system, allowing the closer installation of satellites in orbit.

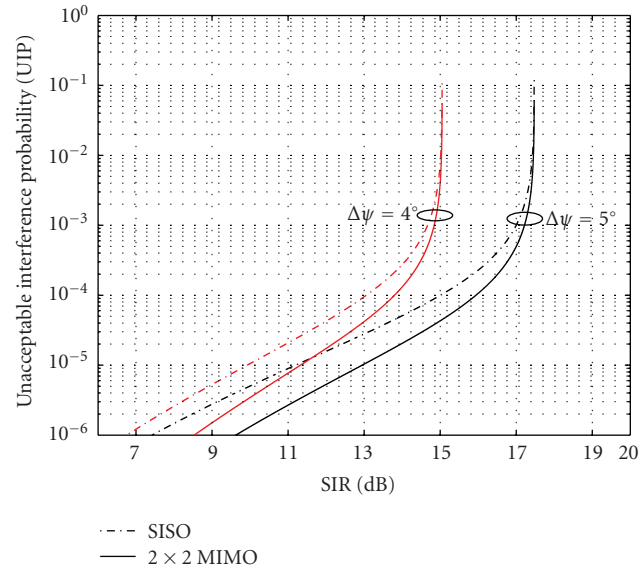

Figure 9: UIP versus SIR for a satellite 2 × 2 MIMO diversity system employing receive antenna selection. Relevant SISO case is also plotted for comparison. Effect of angular separation $\Delta\Psi$.

6. CONCLUSIONS

In this paper, the applicability of MIMO technology to satellite communication systems operating at the Ku-band and above is investigated. Emphasis is put on satellite diversity as a potential candidate to form a MIMO matrix channel in the satellite environment. The relevant propagation phenomena at the frequencies of interest have been considered through an appropriate physical channel model, which takes into account clear LOS operation, high antenna directivity at the TS receiver, the effect of rain fading, and the slant path lengths difference. Also, as it may accept physical inputs from the ITU-R rainmaps, it is flexible and can be applied on a global scale.

Useful *analytical* results are presented for two different applications of MIMO technology:

(i) capacity improvement in a satellite 2×2 MIMO spatial multiplexing system,
(ii) interference mitigation in a satellite 2×2 MIMO diversity system with receive antenna selection.

In the first application, significant capacity gains of the MIMO system over the relevant SISO one are demonstrated, especially for moderate and high SNR levels. The practical case when no CSI is available at the transmitters of the two individual satellites is considered. A useful closed form expression for the outage capacity achieved by 2×2 MIMO satellite systems is provided and successfully verified through Monte Carlo simulations. Such an expression is extremely hard to obtain even in the well-established field of MIMO theory, is applicable over a large SNR range, and can incorporate the effect of various geometrical and operational system parameters on the outage capacity distribution.

In the second application, the receive antenna selection scheme employed in the satellite MIMO system assumed is considered to counteract CCI problems over its forward link. SIR gain of several dB is demonstrated in the numerical results. An analytical propagation model for the calculation of the interference mitigation achieved is presented, which is flexible and can incorporate the influence of various geometrical and operational system parameters on the SIR distribution.

APPENDIX

CALCULATION OF SATELLITE 2×2 MIMO DIVERSITY SYSTEM MARGIN M_d

Every user in the assumed satellite 2×2 MIMO diversity system employing receive antenna selection must comply with a certain availability percentage p_{avail} related to a diversity system margin M_d:

$$\begin{aligned} p_{\text{avail}} \cdot 100\% &= P(\Omega) = P(A_{\text{out}} < M_d) \\ &= P(\min\{A_1, A_2\} < M_d) \\ &= 1 - P(A_1 > M_d, A_2 > M_d) \\ &= 1 - P(A_{R1} > M_d - \text{FSL}_1, A_{R2} > M_d - \text{FSL}_2). \end{aligned} \tag{.1}$$

Considering the transformation given in (8), relating the log-normal rain attenuation RVs A_{Ri} $(i = 1, 2)$ to the normalized normal RVs u_i $(i = 1, 2)$, and the channel modeling assumptions, p_{avail} is expressed as

$$p_{\text{avail}} \cdot 100\% = 1 - \int_{u_{F1}}^{+\infty} du_1 \int_{u_{F2}}^{+\infty} du_2 f_{U_1U_2}(u_1, u_2), \tag{.2}$$

where

$$u_{Fi} = \frac{[\ln((M_d - FSL_i)\cos\phi_i) - \ln(A_{m_{Ri}})]}{S_{a_{Ri}}} \quad (i = 1, 2). \tag{.3}$$

After straightforward algebra, (.2) yields

$$p_{\text{avail}} \cdot 100\% = 1 - 0.5 \int_{u_{F1}}^{+\infty} du_1 \, f_{U_1}(u_1) \operatorname{erfc}\left(\frac{u_{F2} - \rho_{n12}u_1}{\sqrt{2(1-\rho_{n12}^2)}}\right). \tag{.4}$$

ACKNOWLEDGMENTS

The authors are indebted to the three anonymous reviewers whose constructive comments helped to significantly improve the initial version of this paper. Moreover, the first author would like to thank Professor Bhaskar D. Rao from University of California, San Diego, USA, for the fruitful discussions they had on the first part of this work.

REFERENCES

[1] A. J. Paulraj, D. A. Gore, R. U. Nabar, and H. Bölcskei, "An overview of MIMO communications—a key to gigabit wireless," *Proceedings of the IEEE*, vol. 92, no. 2, pp. 198–218, 2004.
[2] D. Gesbert, M. Shafi, D.-S. Shiu, P. J. Smith, and A. Naguib, "From theory to practice: an overview of MIMO space-time coded wireless systems," *IEEE Journal on Selected Areas in Communications*, vol. 21, no. 3, pp. 281–302, 2003.
[3] A. D. Panagopoulos, P.-D. M. Arapoglou, and P. G. Cottis, "Satellite communications at Ku, Ka, and V bands: propagation impairments and mitigation techniques," *IEEE Communications Surveys and Tutorials*, vol. 6, no. 3, pp. 2–14, 2004.
[4] K. P. Liolis, A. D. Panagopoulos, and P. G. Cottis, "Outage capacity statistics of MIMO satellite networks operating at Ka band and above," in *Proceedings of the 12th Ka and Broadband Communications Conference*, Naples, Italy, September 2006.
[5] F. Yamashita, K. Kobayashi, M. Ueba, and M. Umehira, "Broadband multiple satellite MIMO system," in *Proceedings of the 62nd IEEE Vehicular Technology Conference (VTC '05)*, pp. 2632–2636, Dallas, Tex, USA, September 2005.
[6] P. R. King and S. Stavrou, "Land mobile-satellite MIMO capacity predictions," *Electronics Letters*, vol. 41, no. 13, pp. 749–751, 2005.
[7] T. Hult and A. Mohammed, "MIMO antenna applications for LEO satellite communications," in *Proceedings of the 3rd ESA International Workshop of the European COST 280 Action*, Prague, Czech Republic, June 2005.
[8] C. Martin, A. Geurtz, and B. Ottersten, "Spectrally efficient mobile satellite real-time broadcast with transmit diversity," in *Proceedings of the 60th IEEE Vehicular Technology Conference (VTC '04)*, vol. 6, pp. 4079–4083, Los Angeles, Calif, USA, September 2004.
[9] C. Faller, B.-H. Juang, P. Kroon, H.-L. Lou, S. A. Ramprashad, and C.-E. W. Sundberg, "Technical advances in digital audio radio broadcasting," *Proceedings of the IEEE*, vol. 90, no. 8, pp. 1303–1333, 2002.
[10] J. Mietzner and P. A. Hoeher, "Distributed space-time codes for cooperative wireless networks in the presence of different propagation delays and path losses," in *Proceedings of Sensor Array and Multichannel Signal Processing Workshop (SAM '04)*, pp. 264–268, Barcelona, Spain, July 2004.
[11] B. N. Getu and J. B. Andersen, "The MIMO cube—a compact MIMO antenna," *IEEE Transactions on Wireless Communications*, vol. 4, no. 3, pp. 1136–1141, 2005.

[12] I. Frigyes and P. Horváth, "Polarization-time coding in satellite links," *IEEE Satellite and Space Communications Newsletter*, vol. 15, no. 2, pp. 6–8, 2005.

[13] P. Horváth and I. Frigyes, "SAT02-6: application of the 3D polarization concept in satellite MIMO systems," in *Proceedings of IEEE Global Telecommunications Conference (GLOBECOM '06)*, pp. 1–5, San Francisco, Calif, USA, November 2006.

[14] P. R. King and S. Stavrou, "Capacity improvement for a land mobile single satellite MIMO system," *Antennas and Wireless Propagation Letters*, vol. 5, no. 1, pp. 98–100, 2006.

[15] M. Sellathurai, P. Guinand, and J. Lodge, "Space-time coding in mobile satellite communications using dual-polarized channels," *IEEE Transactions on Vehicular Technology*, vol. 55, no. 1, pp. 188–199, 2006.

[16] G. Taricco, E. Viterbo, and E. Biglier, "MIMO transmission for mobile satellite communication systems: a review," in *Proceedings of the 8th International Workshop on Signal Processing for Space Communications (SPSC '03)*, Catania, Italy, September 2003.

[17] A. D. Panagopoulos and J. D. Kanellopoulos, "Prediction of triple-orbital diversity performance in Earth-space communication," *International Journal of Satellite Communications*, vol. 20, no. 3, pp. 187–200, 2002.

[18] ITU-R Recommendation P.837-4, "Characteristics of Precipitation for Propagation Modeling," Geneva, Switzerland, 2003.

[19] G. J. Foschini and M. J. Gans, "On limits of wireless communications in a fading environment when using multiple antennas," *Wireless Personal Communications*, vol. 6, no. 3, pp. 311–335, 1998.

[20] I. E. Telatar, "Capacity of multi-antenna Gaussian channels," *European Transactions on Telecommunications*, vol. 10, no. 6, pp. 585–595, 1999.

[21] S. Sanayei and A. Nosratinia, "Antenna selection in MIMO systems," *IEEE Communications Magazine*, vol. 42, no. 10, pp. 68–73, 2004.

[22] J. D. Kanellopoulos, S. Ventouras, and C. N. Vazouras, "A revised model for the prediction of differential rain attenuation on adjacent Earth-space propagation paths," *Radio Science*, vol. 28, no. 6 part 2, pp. 1071–1086, 1993.

[23] P.-D. M. Arapoglou, A. D. Panagopoulos, J. D. Kanellopoulos, and P. G. Cottis, "Intercell radio interference studies in CDMA-based LMDS networks," *IEEE Transactions on Antennas and Propagation*, vol. 53, no. 8, pp. 2471–2479, 2005.

[24] A. D. Panagopoulos, P.-D. M. Arapoglou, J. D. Kanellopoulos, and P. G. Cottis, "Intercell radio interference studies in broadband wireless access networks," *IEEE Transactions on Vehicular Technology*, vol. 56, no. 1, pp. 3–12, 2007.

[25] ITU-R Recommendation S.580-6, "Radiation Diagrams for Use as Design Objectives for Antennas of Earth Stations Operating with Geostationary Satellites," Geneva, Switzerland, 2004.

[26] P. Horváth and I. Frigyes, "Application of the MIMO concept in millimeter-wave broadband wireless access networks," *International Journal of Wireless Information Networks*, vol. 11, no. 4, pp. 217–225, 2004.

[27] A. Papoulis and S. U. Pillai, *Probability, Random Variables and Stochastic Processes*, McGraw-Hill, Englewood Cliffs, NJ, USA, 4th edition, 2002.